DOI: 10.24996/ijs.2026.67.11.30

ISSN: 0067-2904

A Comparative Study of Satellite Galaxies in the Milky Way and Andromeda

Ahmed H. Abdullah[1,*] Layali Y. Salih [2]
[1]*Department of Astronomy and Space, College of Science, University of Baghdad, Baghdad, Iraq.*
[2]*Department of Applied Mathematics, Mälardalen University, Sweden.*

Received: 16/6/2025 Accepted: 18/1/2026 Published: xx

Abstract

We investigate satellite galaxies orbiting the Milky Way (MW) and Andromeda galaxies (M31). This provides new and important information about the evolutionary history of galaxies in the Local Group. We study the dynamics of these galaxies, stellar mass, luminosity, and metallic composition to reveal changes resulting from their formation history and the influences of their surrounding environment. The stellar mass distribution of the M31's satellites shows a clear tendency for them to be more massive than those of the MW's satellites, despite the general similarity in metallicity distributions. This may be due to more efficient star formation in the early stages or because some star formation processes were less affected by tidal disruption. The Andromeda's satellites exhibit a clear gradient in mass and metallicity composition, indicating the influence of external environments. Furthermore, the M31 system shows a wider variation in the relationship between absolute magnitude and stellar mass, which may indicate a more complex dynamic history resulting from additional mergers and dynamic friction. These results are consistent with the environmental framework that the host galaxy uses to influence the properties of its satellite galaxies, and demonstrate important cosmological constraints.

Keywords: Galaxies' formation, Galaxies' evolution, Satellite galaxy, Local Group

دراسة مقارنة للأقمار التابعة لمجرتي درب التبانة وأندروميدا

أحمد حسن عبد الله[1*] , ليالي يحيى صالح[2] ,
[1] قسم الفلك والفضاء، كلية العلوم، جامعة بغداد، بغداد، العراق
[2]قسم الرياضيات التطبيقية، جامعة مالاردالن، السويد

الخلاصه:

نُجري دراسةً للمجرات التابعة التي تدور حول مجرتي درب التبانة (MW) وأندروميدا (M31) يُوفر هذا معلوماتٍ جديدةً وهامةً حول التاريخ التطوري للمجرات في المجموعة المحلية. ندرس ديناميكيات هذه المجرات، وكتلتها النجمية، ولمعانها، وتركيبها المعدني، للكشف عن التغيرات الناتجة عن تاريخ تكوينها وتأثيرات بيئتها المحيطة. يُظهر توزيع الكتلة النجمية للمجرة التابعة لأندروميدا ميلًا واضحًا نحو أن تكون أضخم من تلك الموجودة في المجرة التابعة لمجرة درب التبانة، على الرغم من التشابه العام في توزيعات المعدنية. قد يُعزى ذلك إلى تكوين النجوم بكفاءةٍ أكبر في المراحل المبكرة، أو لأن بعض عمليات تكوين النجوم كانت أقل تأثرًا بالتمزق

*Email: : ahmed.h.abdullah@sc.uobaghdad.edu.iq

Open Access Articles. This articles is licensed under

المدّي. تُظهر المجرة التابعة لأندروميدا تدرجًا واضحًا في الكتلة والتركيب المعدني، مما يُشير إلى تأثير البيئات الخارجية. علاوةً على ذلك، يُظهر نظام أندروميدا تباينًا أوسع في العلاقة بين القدر المطلق والكتلة النجمية، مما قد يُشير إلى تاريخ ديناميكي أكثر تعقيدًا ناتج عن عمليات اندماج إضافية واحتكاك ديناميكي. تتفق هذه النتائج مع الإطار البيئي الذي تستخدمه المجرة المضيفة للتأثير على خصائص مجراتها التابعة، وتوضح قيودًا كونية مهمة.

1. Introduction

Satellite galaxies (SGs) are important indicators for understanding the hierarchical structure and evolutionary processes of giant galaxies. The MW and M31 galaxies host numerous satellite systems, providing a unique opportunity to study their chemical and dynamic history. However, the disparate environmental conditions and assembly histories imply varying evolutionary paths. The equivalent abundance of SGs in both systems indicates similarities in the processes for satellite evolution [1, 2].

This study aims to describe and contrast the MW and M31 satellite galaxies in terms of the stellar mass, metallicity, luminosity, and kinematic properties. The distributions of metallicity are different, and the contrast, however subtle, may indicate differing star formation processes in the early phases, varying gas infall histories, and disparate enrichment processes [3].
Recent studies have challenged the assumption of isotropy in satellite distributions under ΛCDM cosmology [4]. Studies [5,6] identified coherent planar structures surrounding both MW and M31, indicating possible anisotropic accretion along cosmic filaments or remnants of early mergers. In fact, the SGs seem to follow the direction of the large-scale cosmic web [7, 8, 9], but the MW's satellite plane seems to be out of alignment with M31's web-aligned arrangement [10, 11].

Even at large galactocentric radii, kinematic studies show that satellite velocity dispersion scales with star mass and proximity to the host galaxy, indicating the impact of ram-pressure stripping and tidal stirring [12]. By allowing cross-comparisons between satellite systems in galaxies of similar mass, the ELVES Survey [13] has broadened the contextual background and brought attention to the influence of local environmental histories on satellite demography.

Furthermore, satellite galaxies have prolonged quiescence interspersed with periodic bursts, according to star formation histories deduced from color–magnitude diagrams and surface brightness profiles [14]. Under a range of cosmological feedback conditions, theoretical models such as " FIRE-2 and AURIGA simulations " have supported observable scaling relations, including the magnitude velocity dispersion correlation and the mass-to-metallicity trend [15, 16, 17].

The objective of this study is to provide a data-driven, comparative investigation of the kinematic, chemical, and photometric characteristics of satellite galaxies associated with M31 and MW. We investigate how the evolutionary fates of these satellites are influenced by variations in host galaxy characteristics and assembly paths. The structure of the paper is as follows: Section 2 describes data acquisition and preprocessing; Section 3 analyzes stellar mass and metallicity distributions, luminosity –mass correlations, and also discusses spatial and kinematic structures. Section 4 presents the main conclusions.

2. The Sample and Dataset

This study uses a meticulously prepared gain basis list of 40 satellites gravitionally bound to the MW, M31, considering the MW satellites with heliocentric distances under 400 kpc, and the M31 satellites with projected distances within 450 kpc of their host. For reliable stellar mass and metallicity measurements, systems fainter than Mv = - 5 were excluded.
Only galaxies with well-constrained stellar mass, metallicity ([Fe/H]), absolute magnitude, effective radius, and velocity dispersion were retained.

The physical parameters were compiled from available databases, including the SIMBAD Astronomical Database (CDS, Strasbourg; https://sim-bad.cds.unistra.fr/simbad), the Strasbourg Astronomical Center (https://cds.unistra.fr), and the NASA/ IPAC Extragalactic Database (https://nad.ipac.caltech.edu).
Because the data originated from multiple sources, all parameters were homogenized prior to analysis. Stellar masses were converted to a common scale assuming a Chabrier initial mass function (IMF) [18]. Metallicity values reported on different calibration scales were transformed to a unified [Fe/H] scale following [19]. Distance and absolute magnitude were recalculated using consistent distance moduli for both host galaxies, 8.2 kpc for the MW and 780 (kpc) for M31, and effective radii were adopted from the surface brightness profile.

The final dataset contains, for each satellite, galactic coordinates, morphological classification, stellar mass, absolute magnitude, surface brightness, metallicity, stellar population age, velocity dispersion, and heliocentric distance. All parameters were standardized and stored in FITs format, the widely adopted data standard in observational astronomy. Using standard tools for reading and manipulating FIT files, the dataset was then analyzed and visualized in the R statistical computing environment. These results aid in a comparative analysis of the stellar, chemical, and dynamic properties of the MW and MW satellite systems.

3. Results and discussion

The formation and dynamical patterns of satellite systems around the MW and the M31 offer important insights into galaxy evolution in diverse galactic environments. High-resolution models [20] suggest that the varying properties of satellite galaxies may be influenced by the host galaxy's mass, surrounding environmental impacts, star-forming feedback, and the history of galaxy mergers. Here, we focus on the distribution of stellar mass and metallicity in satellite systems of the MW and M31, along with some other important physical parameters.

3.1 Milky Way and Andromeda satellites' stellar mass and metallicity distributions.

The mass distribution of stars in the satellite galaxies MW and M31 is shown in the left panel of Figure 1. The distributions reveal considerable differences in the star mass range and frequency between the two host galaxies. The M31 satellites in orange exhibit a wider distribution with a higher mean stellar mass, while the MW satellites in blue show a steeply peaked distribution with a larger concentration of low-mass systems. According to the trend, there is a relatively higher percentage of enormous systems in the M31 satellite community compared to MW, which is consistent with the results of previous studies (e.g. [21, 22]). These variations are further highlighted by the kernel density estimation curves, which show longer tails for the M31 satellites as their stellar mass increases. The dashed vertical lines, which represent the average mass for each host system, demonstrate the variation in typical satellites' mass.
According to average values, the M31 satellites are frequently heavier than their MW counterparts. This discrepancy may be due to fundamental differences in the formation pathways of the satellites' systems, variations in the accretion history, or the environmental efforts [23].

The stellar mass distribution of the MW and M31 satellites is shown as a box plot in the right panel of Figure 1. The median results support the difference in the histogram, indicating that M31 has a higher median stellar mass. Furthermore, there is a greater variety in star mass among the population, as seen by the wider middle 50% range of the M31 satellites. A few galaxies stand out from the overall distribution, especially in the M31 sample, indicating the presence of a few very large satellites. These might include systems with relatively high star masses, as M32 or NGC205 [24].

The general trend is supported by the mean values indicated by the red dots in Figure 1; on average, M31 spacecraft are heavier than MW satellites. This discrepancy could be the result of contrasting evolutionary paths, with M31 most likely undergoing a more substantial accretion or merging event. In line with the hypothesis that some galaxies maintain abnormally high stellar masses due to either intense early star formation or more effective gas retention, both systems are well outside of the ordinary range [25].
We applied the Mann-Whitney U (MWU) and Kolmogorov-Smirnov (KS) tests to statistically test these differences (Table 1).

Table 1: shows the statistical comparison of the M31 and MW satellites' stellar mass distributions.

Test	Statistic	p-value
Kolmogorov-Smirnov	D = 0.390	0.0929
Mann-Whitney U	U = 99.0	0.0183

The Mann-Whitney U test shows a statistically significant difference in the ranking distributions (U=99.0, p = 0.0183); however, the KS test produces findings that are marginally non-significant (D = 0.390, P = 0.0929). Together, the results support the interpretation that M31 satellites are generally more massive than MW satellites, which is consistent with the visual evidence presented in Figure 1. The contrasting stellar mass distribution of MW and M31 satellites highlights distinct evolutionary pathways. The dominance of low-mass satellites in the MW suggests stronger suppression of star formation, likely driven by environmental processes such as ram pressure stripping or tidal interactions [26].

In Figure 2, you can see a comparison of the [Fe/H] ratios for the MW and M31 satellite galaxies for their respective metallicity distributions. Although both systems encompass broadly similar ranges of metallicity, the mean [Fe/H] values differ. While the mean metallicity of the MW is -2.03, M31 is -1.76. This observation suggests that the M31 satellites are, on average, more metal-rich. While the difference is modest (~0.27 dex), it might still be due to differences in accretion histories or to differences in the efficiencies of star formation and the feedback in the two systems.

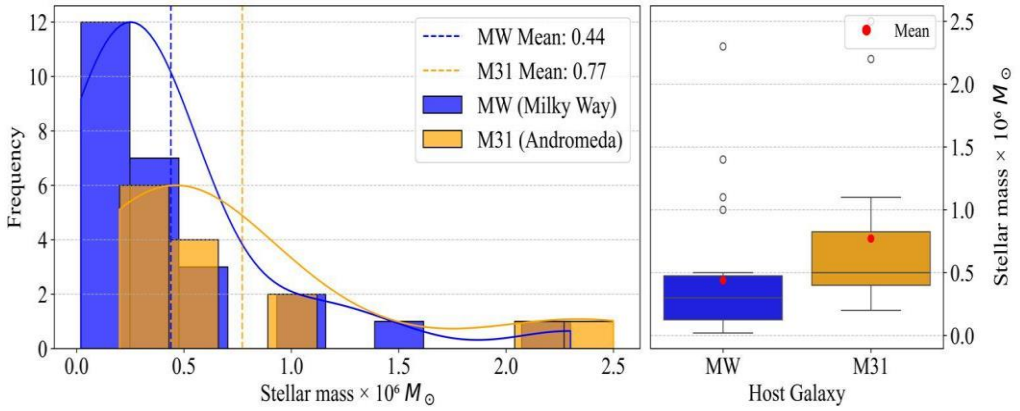


Figure 1: Comparative analysis of stellar mass distributions of the MW (blue) and M31 (orange) systems. The difference in average stellar mass for M31 and MW satellite galaxies, 0.77×10^6 $M_\odot$ and 0.44×10^6 $M_\odot$,respectively, the difference in mass distribution and diversity can be seen on the left. However, the right panel supports the statement on the more hierarchical universe toward M31, underlined by the greater median mass and increased interquartile range shown on M31's box plot.

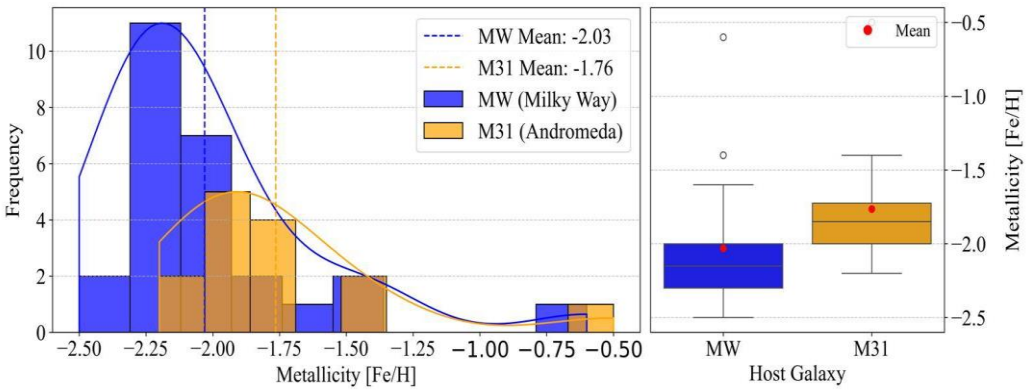


Figure 2: The metallicity distributions of satellites across the MW (blue) and M31 (orange) systems. The left panel shows that Andromeda's satellite galaxies have higher metallicities than those of the Milky Way, signifying a strong chemical contrast (mean [Fe/H] = -1.76 for Andromeda, whereas mean [Fe/H] = -2.03 for the Milky Way). The boxplot in the right panel, which shows the central measures of tendency, depicts the metallicity variation of Andromeda satellites, showing that Andromeda has greater diversity in its metallicity. This provides strong evidence that the two systems underwent different chemical enrichment processes.

The histograms cover the range of [Fe/H] values from -2.50 to -0.50, with most of the satellites clustered between -2.00 and -1.50. Both systems have a peak between -1.75 and -1.50, indicating concentrated distributions, albeit moderately. M31, however, has a slight tendency to higher metallicities, likely the result of more advanced early chemical enrichment. These differences might result from variations in early gas accretion and star formation, along with differing chemical enrichment histories as a result of distinct assembly pathways. The radial metallicity gradient of M31's inner disk (~0.043 dex kpc^{-1}) and nearly uniform α-enhancement in the central region attest to such a complex assembly history and to the spectroscopic observations from APOGEE-integrated spectra [27, 28].

3.2 Absolute magnitude-Stellar mass relationship in Milky Way and Andromeda satellites

In satellite galaxies, the correlation between stellar mass and absolute magnitude illustrates the potential of their dark matter halos and the efficiency of stellar formation. For the M31 and MW systems, we observe a general pattern where more massive satellites tend to be more luminous (as shown in Figure 3). There does, however, seem to be more scatter with the M31 satellites. This could be due to more varied stellar formation histories or more substantial dynamical interactions within the host halo environment. This scatter aligns with the findings of [29], which highlighted the impacts of internal and host-specific interactions on the evolution of satellite systems.

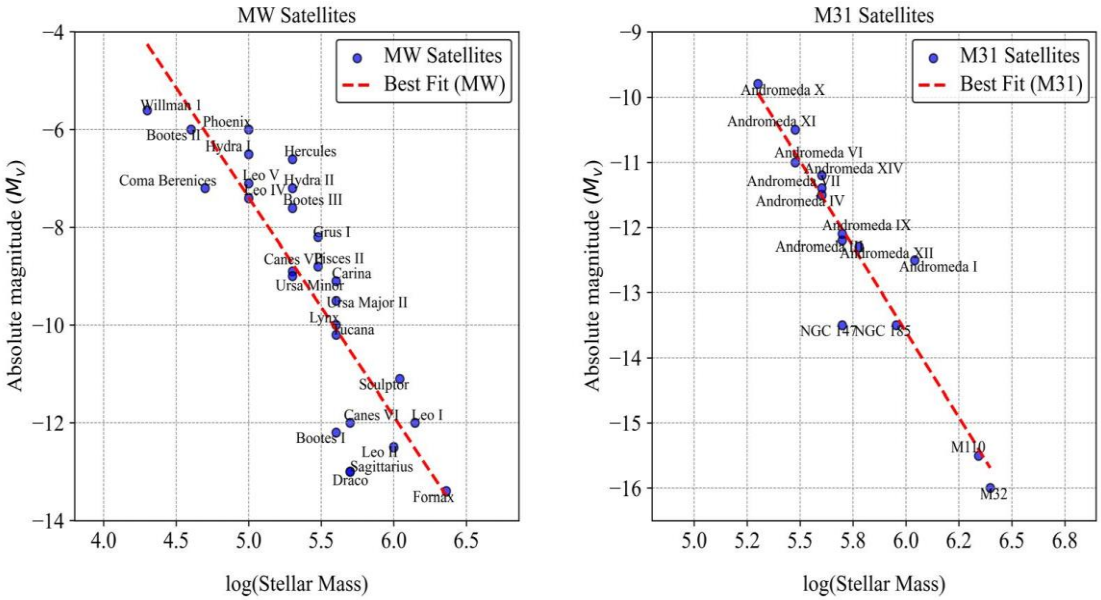


Figure 3: The relationship between absolute magnitude and stellar mass for satellite galaxies in the Milky Way (left) and Andromeda (right) systems. Both populations follow the expected trend of brighter galaxies (lower M_v) possessing higher stellar masses. The red dashed lines represent the best-fit linear trends.

3.3 The mass-metallicity relationship in the MW and M31 satellites

The mass and metallicity relation, in which galaxies with higher stellar mass tend to exhibit greater metal enrichment. It is well established and reflects the capacity of massive systems to retain metals due to deeper potential wells and reduced susceptibility to outflows. In the MW and M31 satellite systems, there is a clear trend. However, satellites of M31 display a marginally steeper mass–metallicity relation slope compared to their MW counterparts, possibly indicating stronger environmental quenching or differences in their initial gas content and feedback history [30]. Figure 4 illustrates the mass-metallicity relation for the two satellite populations, showing a systematically higher metal retention in more massive galaxies, with M31 satellites trending toward lower metallicities at fixed mass.

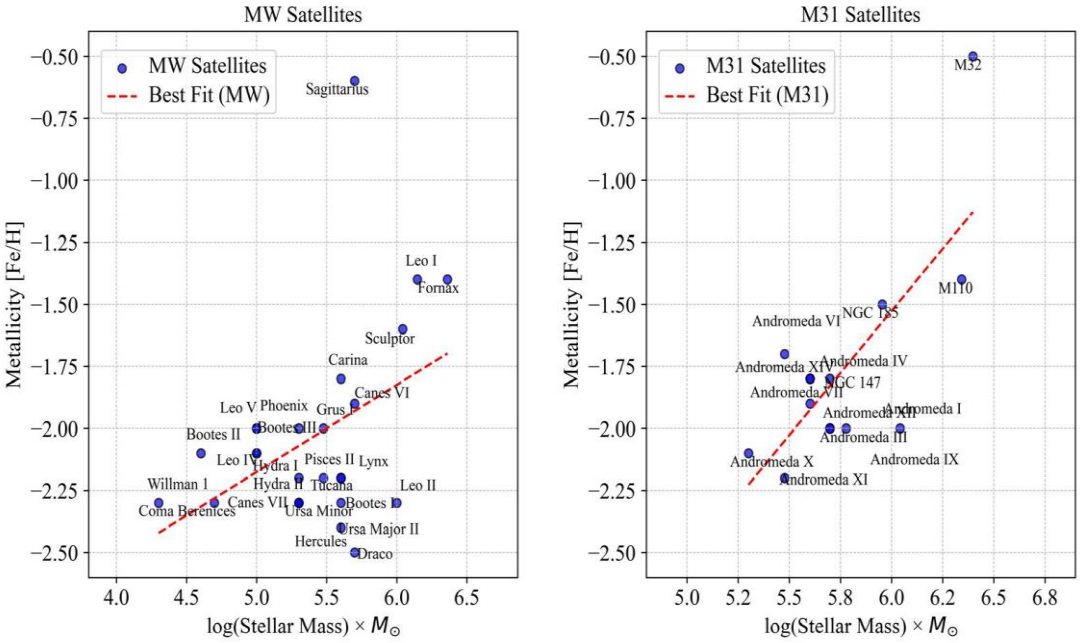


Figure 4: A comparative analysis of the mass-metallicity relation within the satellite galaxies of the Milky Way (left) and Andromeda (right). Both systems independently affirm the foundational principle that higher stellar mass correlates with greater metal enrichment. The red dashed lines represent the best-fit linear trends.

3.4 Kinematic Properties: Velocity Dispersion and Effective Radius

The relationship between a satellite's velocity dispersion (σ) and effective radius (R_e) is powerful. It can diagnose the underlying gravitational potential, the dynamical history, and the history of the satellite. The pronounced scatter observed at comparable stellar masses highlights the restrictions of mass as the only metric upon which to base the kinematic state. The scatter is a natural prediction of the ΛCDM cosmology, which is the dark matter halo concentration and its imprinting upon the internal dynamics of the stellar kinematics. For a satellite residing in a more concentrated halo, or one that has suffered less tidal heating, one would expect higher velocity dispersion relative to the given physical size. The observation that M31 satellites show more dispersion in this section of parameter space is particularly evident in their over-representation of systems with high values of σ at low R_e. AURIGA and other simulations show that satellites that have been accreted in groups or along more radial orbits experience greater tidal stirring as well as ram-pressure stripping. These mechanisms lead to the efficient clearing of the outer envelope of a galaxy of loosely bound stars so that R_e is reduced, and the denser, dynamically hot core is left intact, thus increasing the central velocity dispersion. The kinematic diversity of M31's population is thus a likely fossil record of the environmentally driven transformation.

The link between a satellite's effective radius (R_e) and velocity dispersion (σ) is shown in Figure 5 and is a powerful indicator of its dynamical history and underlying gravitational potential. The significant dispersion seen at similar stellar masses highlights how mass alone is not a reliable indicator of kinematic condition. The ΛCDM cosmology naturally predicts this heterogeneity, where the internal kinematics of the star component are imprinted by the dark matter halo concentration. For a given physical size, satellites that live in more concentrated halos or those that have not been heated by tidal waves will naturally show larger velocity dispersions. [31]

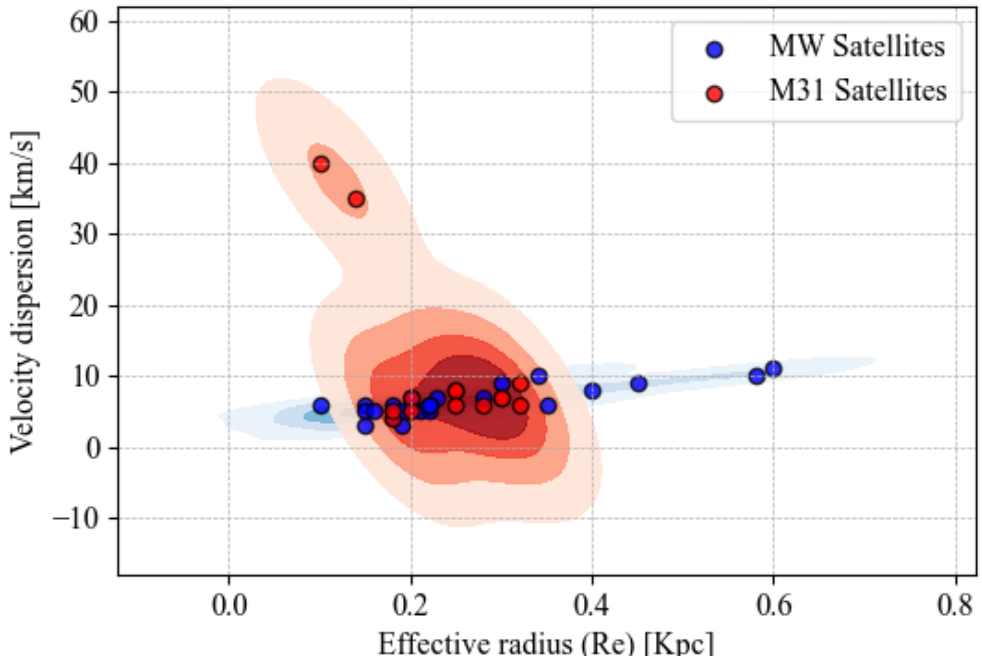


Figure 5: Relationship between the velocity dispersion and the effective radius for satellite galaxies of the Milky Way and Andromeda, depicted via density contours.

3.5 Velocity Dispersion of Satellite galaxies in the Milky Way and Andromeda satellites

Figure 6 presents the velocity dispersions of satellite galaxies in the MW and M31. Most satellites in both systems have modest dispersions (≤ 10 km s -1). M31 exhibits a broader upper tail driven by a few high-dispersion objects. To move beyond visual comparison and mean values, we again apply the two-sample Kolmogorov-Smirnov (KS) test to compare the overall distributions and the two-sided Mann-Whitney U (MWU) test to assess a shift in median shifts (see Table 2).

According to the KS test, there is no difference in the overall shapes, where D = 0.225, p = 0.656, and the rank-based Mann-Whitney test likewise found no shift in the typical values (U = 140, p = 0.231). The sample medians are 6 and 7 km s^{-1} for the MW and M31, respectively. We adopt a conventional two-sided significance threshold of $\alpha = 0.05$, where $p < 0.05$ is treated as statistically significant. Under this criterion, neither test indicates a difference between the MW and M31 velocity dispersion distributions. The estimated effect size is small (Cliff's $\delta = -0.23$), indicating only a slight tendency for MW dispersions to be lower.

Table 2: Statistical comparison of the velocity dispersion distribution of MW vs M31

Test	Statistic	p-value
Kolmogorov-Smirnov	D = 0.225	0.656
Mann-Whitney U	U = 140	0.231
Cliff's delta effect	δ = 0.23	

The heavier M31 tail is consistent with the presence of a handful of dynamically "hot" satellites. For example, the compact elliptical M32 shows central dispersions of ≥ 100 – 175 km s^{-1} in HST/ STIS measurements [32], and the M31 dwarf ellipticals NGC 185 and NGC 147 exhibit average dispersions of ≈ 24 ± 1 and 16 ± 1 km s^{-1}, respectively [33,34].

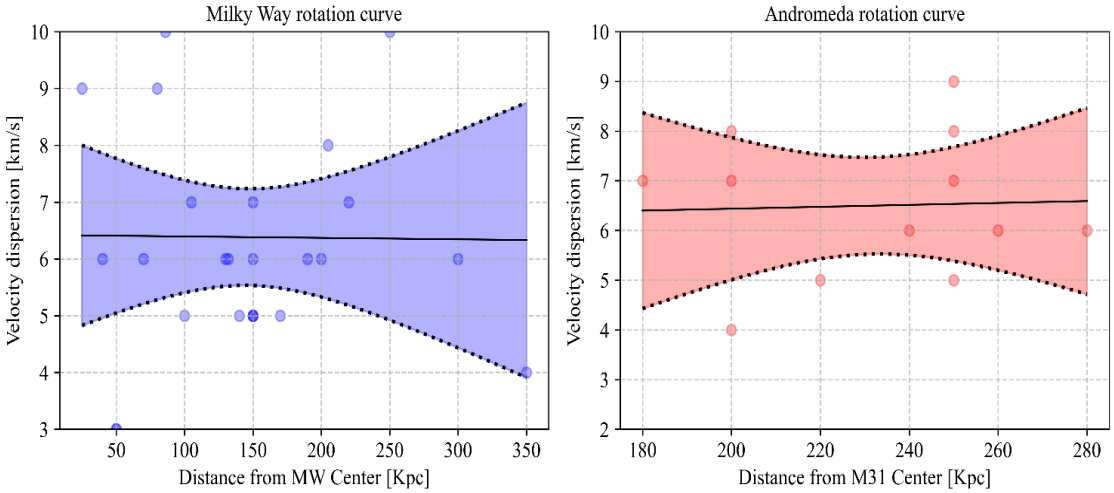


Figure 6: A comparative analysis of the internal velocity dispersions for satellite galaxies as a function of their projected distance from the host galactic centre for the Milky Way (left) and Andromeda (right). Both systems are dominated by satellites with low velocity dispersions ($\leq$ 10 km s^{-1}).

4. Conclusions

This comparative study examines the structural and evolutionary differences between the satellite galaxies of the MW and M31. This study reveals intriguing variations in the kinematics, stellar mass, and metallicity of the satellite galaxy systems. On average, satellite galaxies of the M31 have larger masses than satellite galaxies of the MW. This may be attributed to either more efficient early star formation or less disruptive tidal interactions in the M31's outer halo, compared to the Milky Way. Although the enrichment of the satellites of MW and M31 is generally similar, the M31 satellite exhibits a steeper mass-metallicity relationship. This suggests that environmental factors, such as the initial gas concentration, ram pressure stripping, and the merger history, become more significant during chemical evolution. The greater dispersion in the absolute magnitude- stellar mass relationship in the M31 satellite likely reflects a more dynamic accretion history resulting from more frequent accretion processes and interactions.

References

[1] K. Wang, "An evolutionary continuum from nucleated dwarf galaxies to star clusters," Nature, vol. 623, no. 7986, pp. 296–300, 2023. doi:10.1038/s41586-023-06650-z.

[2] M. N. Al Najm, O. L. Polikarpova, and Yu. A. Shchekinov, "Ionized Gas in the Circumgalactic Vicinity of the M81 Galaxy Group," Astronomy Reports, vol. 60, pp. 389–396, 2016. doi: 10.1134/S1063773721030014.

[3] S. A. A. Al, M. N. A. H., and H. Huda, "Measurement of the distance to the central stars of Nebulae by using Expansion methods with Alladin Sky Atlas," 1st Int. Conf. Phys. Sci. Adv. Mater., IOP Conf. Ser., vol. 757, 2020. doi: 10.1088/1757-899X/757/1/012043.

[4] Z. J. Xu, "Maximum entropy distributions of dark matter in ΛCDM cosmology," Astronomy and Astrophysics, vol. 675, Art. no. A92, 2023. doi:10.1051/0004-6361/202346429.

[5] M. Metz, P. Kroupa, and H. Jerjen, "The spatial distribution of the Milky Way and Andromeda satellite galaxies," Monthly Notices of the Royal Astronomical Society, vol. 374, no. 3, pp. 1125–1145, 2007. doi:10.1111/j.1365-2966.2006.11228.x.

[6] T. Sawala et al., "The Milky Way's plane of satellites is consistent with Λ CDM," Nature Astronomy, vol. 7, no. 4, pp. 481–491, 2023. doi:10.48550/arXiv.2205.02860.

[7] Q. Gu, "The spatial distribution of satellites in galaxy clusters," Monthly Notices of the Royal Astronomical Society, vol. 514, no. 1, pp. 390–402, 2022. doi:10.1093/mnras/stac1292.

[8] L. Tang, W. Lin, and Y. Wang, "Satellite Alignment. III. Satellite Galaxies' Spatial Distribution and Their Dependence on Redshift with a Novel Galaxy Finder," The Astrophysical Journal, vol. 893, no. 2, Art. no. 87, 2020. doi:10.3847/1538-4357/ab8292.

[9] A. K. Ahmed, G. B. Ali, and M. Y. Amin, "Detailed surface photometry of the spiral galaxies NGC 7339, NGC 7537, and NGC 7541," Int. J. Adv. Res., vol. 2, no. 1, Jan. 2014.

[10] A. Eckart et al., "The infrared K-band identification of the DSO/G2 source from VLT and Keck data," Proceedings of the International Astronomical Union," vol. 9, no. S303, pp. 269–273, 2023. doi: 10.1017/S1743921314000726.

[11] Rashed, Y. E., Zuther, J., Eckart, A., Busch, G., Valencia-S., M., Vitale, M., Britzen, S., & Muxlow, T., "High-resolution observations of SDSS J080800.99+483807.7 in the optical and radio domains: A possible example of jet-triggered star formation." Astronomy & Astrophysics, vol. 558, A5, 2023 https://doi.org/10.1051/0004-6361/201322211

[12] E. Patel and K. S. Mandel, "Evidence for a Massive Andromeda Galaxy Using Satellite Galaxy Proper Motions," The Astrophysical Journal, vol. 948, no. 2, p. 104, 2023. doi:10.3847/1538-4357/acc029.

[13] S. G. Carlsten, J. E. Greene, R. L. Beaton, S. Danieli, and J. P. Greco, "The Exploration of Local Volume Satellites (ELVES) Survey: A Nearly Volume-limited Sample of Nearby Dwarf Satellite Systems," The Astrophysical Journal, vol. 933, no. 1, Art. no. 47, 2022. doi: 10.3847/1538-4357/ac6fd7.

[14] C. Olsen and E. Gawiser, "Searching for Conformity Across Cosmic Time with Local Group and Local Volume Star Formation Histories," The Astrophysical Journal, vol. 943, no. 1, Art. no. 30, 2023. doi:10.3847/1538-4357/acaa39.

[15] P. F. Hopkins et al., "FIRE-3: updated stellar evolution models, yields, and microphysics and fitting functions for applications in galaxy simulations," Monthly Notices of the Royal Astronomical Society, vol. 519, no. 2, pp. 3154–3181, Feb. 2023. doi:10.1093/mnras/stac3489.

[16] M. N. Al Najm, A. H. A, and Y. E. Rashed, "Estimating the evolution and the content fractions of baryonic gas for Luminous Infrared Galaxies," Mon. Not. R. Astron. Soc., vol. 537, no. 2, pp. 1597–1607, 2025. doi: 10.1093/mnras/staf023.

[17] L. Y. S. Al-Mashhadani and A. H. Abdullah, "A cosmological view for the time-variation of the fundamental constants of nature," NeuroQuantology, vol. 18, no. 12, 2020. doi:10.14704/nq.2020.18.12.NQ20233.

[18] Chabrier, G. (2003). Galactic Stellar and Substellar initial Mass Function. Publication of the Astronomical Society of the Pacific, 115(809), 763-795. https://doi.org/10.1086/376392

[19] Carretta, E., Bragaglia, A., Gratton, R. G., D'Orazi, V., & Lucatello, S. (2009). Na-O anticorrelation and HB. V. the overall metallicity of globular clusters. Astronomy & Astrophysics, 508(2), 695-706. https://doi.org/10.1051/004-6361/200912096

[20] S. Khoperskov, I. Minchev, N. I. Libeskind, M. Haywood, P. Di Matteo, V. Belokurov, M. Steinmetz, F. A. Gómez, R. J. J. Grand, Y. Hoffman, A. Knebe, J. G. Sorce, M. Sparre, E. Tempel, and M. Vogelsberger, "The stellar halo in Local Group Hestia simulations I. The in-situ component and the effect of mergers," Astronomy & Astrophysics, vol. 665, A92, 2022. doi:10.1051/0004-6361/202244232.

[21] McConnachie, A. W. (2012). The observed properties of dwarf galaxies in and around the Local Group. The Astronomical Journal, 144(1), 4. DOI: 10.1088/0004-6256/144/1/4.

[22] Simon, J. D. (2019). The faintest Dwarf Galaxies. Annual Review of Astronomy and Astrophysics, 57, 375-415. https://doi.org/10.1146/annurev-astro-091918-104453

[23] Wetzel, A. R., Tollerud, E. J., & Weisz, D. R. (2015). Rapid environmental quenching of satellite dwarf galaxies in the Local Group. The Atronomical Journal Letters, 808(1). L27. https://doi.org/10.1088/2041-8205/808/1/L27

[24] Collins, M. L. M., Read, J. I., Ibata, R. A., Rich, R. M., Martin, N. F., Penarrubia, J., Chapman, S. C., Tollerund, E. J., & Weisz, D. R. (2021). Andromeda XXI- a dwarf galaxy in low density dark matter halo. Monthly Notice of Royal Astronomical Society, 505(4), 5686-5701. https://doi.org/10.1093/mnras/stab1624

[25] Kirby, E. N., Cohen, J. G., Guhathakurta, P., Cheng, L., Bullock, J. S., & Gallazzi, A. (2013). The universal stellar mass-stellar metallicity relation of dwarf galaxies. The Astrophysical Journal, 779(2), 102. DOI 10.1088/0004-637X/779/2/102

[26] Fillingham, S. P., COOPER, M. C., Pace, A. B., Boylan-Kolchin, M., Bullock, J. S., Garrison-Kimmel, S., & Wheeler, C. (2016). Under pressure: Quenching star formation in low mass satellite galaxies via stripping. Monthly Notice of Royal Astronomical Society, 463(2), 1916-1928. https://doi.org/10.1093/mnras/stw2131

[27] B. J. Gibson, "The Chemodynamics of the Stellar Populations in M31 from APOGEE Integrated-light Spectroscopy," The Astrophysical Journal, vol. 952, no. 1, Art. no. 23, 2023. doi:10.3847/1538-4357/acd9a9.

[28] A. C. Mason, "Chemical tagging with APOGEE, MUSE, and HST: constraints on the formation of $ω$ Centauri," arXiv e-prints, Art. no. arXiv:2504.06341, 2025. doi:10.48550/arXiv.2504.06341.

[29] H. B. Akins, "Quenching Timescales of Dwarf Satellites around Milky Way-mass Hosts," The Astrophysical Journal, vol. 909, no. 2, Art. no. 139, 2021. doi:10.3847/1538-4357/abe2ab.

[30] M. Damle et al., "Cold and hot gas distribution around the Milky-Way – M31 system in the HESTIA simulations," Monthly Notices of the Royal Astronomical Society, vol. 512, no. 3, pp. 3717–3737, May 2022. doi:10.1093/mnras/stac663.

[31] R. Mallick, S. Singh, and R. Nandi, "Maximum mass of hybrid star formed via shock-induced phase transition in cold neutron stars," Monthly Notices of the Royal Astronomical Society, vol. 503, no. 4, pp. 4829–4837, June 2021. doi:10.1093/mnras/stab417.

[32] Joseph, C. L., Merritt, D., Olling, R., Valluri, M., Bender, R., & Ajhar, E. A. (2001). The nuclear dynamics of M32. I. Data and stellar kinematics. The Astrophysical Journal, 550(2), 668-680. https://doi.org/10.1086/319781

[33] Geha, M., van der Marel. R. P., Guhathakurta, P., Gilbert, K. M., Kalirai, J., & Kirby, E. N. (2010). Local Group dwarf elliptical galaxies. II. Stellar kinematics to large radii in NGC 147 and NGC 185. The Astrophysical Journal, 711(1), 361-373. https://doi.org/10.1088/0004-637X/711/1/361

[34] K. J. Kanehisa, M. S. Pawlowski, and N. Libeskind, "Andromeda's asymmetric satellite system as a challenge to cold dark matter cosmology," Nature Astronomy, vol. 9, pp. 692–701, 2025. doi:10.1038/s41550-025-02480-3.